INFLUENCES OF ALLOY COMPOSITION AND SCRATCHING DEPTHS ON THE DEFORMATION BEHAVIOR OF $FeNiCoCrCu_x$ HIGH-ENTROPY ALLOYS UNDER NANOINDENTATION AND NANOSCRATCH

Pham Van Trung[1]*, Luu Duc Binh[1], Tao Quang Bang[1], Nguyen Van Tho[1], Tu Quang Duc[1]

The University of Danang - University of Science and Technology, Danang, Vietnam

*Corresponding author: pvtrung@dut.udn.vn

(Received: April 30, 2025; Revised: June 15, 2025; Accepted: June 20, 2025)

DOI: 10.31130/ud-jst.2025.23(9B).508E

Abstract - The influence of alloy composition and scratching depth in terms of mechanical properties and microstructural changes of FeNiCoCrCu high-entropy alloys (HEAs) is investigated and evaluated through nanoindentation and nanoscratch techniques via molecular dynamics (MD). The influence of these factors is analyzed by investigating applied force, atomic shear deformation, microstructural alterations, dislocation behavior, and elastic restoration capacity. It is highlighted that the primary mode of deformation throughout the indentation and scratching of FeNiCoCrCu alloys involves the initiation and spread of dislocations and stacking faults. The forces during indentation and scratching generally rise with decreasing Cu content and increasing scratch depth. Additionally, the displacement of atoms in diverse directions results in distinct pile-up morphologies.

Key words - Nanoindentation; nanoscratch; high entropy alloy; molecular dynamics; deformation mechanism

1. Introduction

High-entropy alloys (HEAs), often described as multi-component systems, contain five or more constituent elements with comparable atomic percentages [1]. Despite comprising diverse metallic elements, HEAs typically develop a single-phase solid solution with a straightforward crystal lattice, such as face-centered cubic (FCC) or body-centered cubic (BCC) structures, instead of intricate intermetallic compounds [2-3]. HEAs display remarkable mechanical properties stemming from the pronounced solid-solution strengthening and the presence of diverse deformation mechanisms that mitigate strain concentration and damage [4-5]. These characteristics encompass elevated strength, significant hardness, superior wear resistance, remarkable corrosion resistance, and excellent oxidation resistance [6]. Thanks to their outstanding properties, HEAs are promising materials for use as coatings to enhance the wear resistance of machine components and extend the lifespan of parts [7]. Consequently, numerous researchers have investigated the microstructure and mechanical properties of diverse HEA systems. The remarkable properties of HEAs position them as potential candidates for a range of applications, including fracture-resistant materials, tooling materials, and radiation-resistant materials. Within the family of high-entropy alloys (HEAs), the $FeNiCoCrCu_x$ system has garnered considerable attention from experts owing to its exceptional mechanical characteristics. The $FeCoCrNiCu_x$ HEAs are recognized for their excellent thermal endurance, significant hardness as well as superior wear durability [8-10]. Furthermore, extensive studies have been conducted to investigate the impact of microstructure on the material properties and mechanical behavior of $FeNiCoCrCu_x$ HEAs. Its microstructural characteristics have been thoroughly investigated in prior studies. For instance, Deluigi et al. [11] explored the radiation tolerance of a five-element equiatomic FCC $FeNiCrCo\text{-}Cu_x$ alloy, focusing on how its chemical complexity contributes to reduced thermal conductivity and unique defect behavior. Their study of radiation damage during the initial stage (within 0.1 ns) revealed that the mean defect count generated within the HEA material is consistently smaller compared to that in conventional metals. This result supports previous findings that high-entropy alloys (HEAs) exhibit enhanced tolerance to irradiation. Pham et al. [12] examined how variations in punch angle, temperature, and loading velocity affect the mechanical response of nanoimprinted $FeNiCoCrCu_x$ high-entropy alloys, aiming to elucidate the material's mechanical behavior and deformation mechanisms during the nanoimprinting process, thereby supporting the advancement of its functional applications. Luo et al. [13] explored the distinctive mechanical behavior and evolution of internal structure of the FeCoCNiCu high-entropy alloy, comparing its performance with that of traditional metallic systems through indentation experiments. Their findings showed that the interplay of dislocations with solute atoms, combined with the substantial accumulation of dislocations in the $FeCoCrNiCu_x$ HEA, leads to pronounced strengthening during plastic deformation. Moreover, the alloy's ductility benefits from the activation of various slip systems. Several studies have suggested that the strongest and most efficient alloys do not always exhibit equiatomic composition. Certain studies have shown that the addition of copper (Cu) to the alloy improves its hardness, resistance to oxidation, and wear performance [14]. Conversely, other studies highlight potential drawbacks associated with the addition of Cu [15-16]. Consequently, the contribution of Cu to the alloy significantly influences the material's mechanical behavior. Examining the effect of copper content is crucial for identifying the most suitable material for targeted applications. For this investigation, five distinct compositions, specifically $FeNiCoCrCu_{1.3}$, $FeNiCoCrCu_{1.0}$, $FeNiCoCrCu_{0.7}$, $FeNiCoCrCu_{0.4}$, and $FeNiCoCrCu_{0.2}$ were carefully selected and employed to assess how varying Cu concentrations influence the mechanical performance of $FeNiCoCrCu_x$ high-entropy alloys alloys during both nanoindentation and scratching processes.

Table 1. *Various characteristics of the workpiece examined in this study*

Factor	Characteristic
Material	$FeNiCoCrCu_x$
Dimensions (Å)	130 x 60 x 100
Scratching depth (nm)	0.5, 1.0, 1.5, 2.0
Temperature (K)	300
Loading velocity (m/s)	100
Time step (fs)	1.0
Scratch length (nm)	8.0
Alloy compositions	$FeNiCoCrCu_{1.3}$, $FeNiCoCrCu_{1.0}$, $FeNiCoCrCu_{0.7}$, $FeNiCoCrCu_{0.4}$, $FeNiCoCrCu_{0.2}$

Currently, there is growing attention on investigating the deformation mechanisms of high-entropy alloys (HEAs) through mechanical experiments, including tension [17], compression [18], and indentation [19]. Micromechanical tests primarily offer the benefit of revealing the fundamental properties of materials while minimizing the impact of defects. Standard indentation and scratching methods provide an effective means of assessing mechanical properties, including force, hardness, dislocation behavior, and friction [20]. Using indentation and scratching tests in experimental methods makes it challenging to examine the wear processes and the mechanical behavior of materials on an atomic scale. Besides experimental techniques, molecular dynamics (MD) simulations serve as a powerful tool for uncovering the deformation mechanisms of materials [21-23]. It is commonly employed to examine key deformation behaviors in processes like nanoindentation and nanoscratch testing [24-26]. Zhang et al. [27] explored the mechanical behavior and Hall-Petch phenomenon of the FeNiCoCrCu high-entropy alloy by applying interatomic potentials via molecular dynamics (MD) simulations. Their findings emphasized the correlation between grain size and strength, the deformation processes driven influenced by grain boundaries, and the role of dislocation motions. While previous research has extensively explored the characteristics of the FeNiCoCrCu HEA, including its structure and thermal stability, the fundamental mechanisms behind plastic deformation, specific material behaviors, and the origins of early dislocation sites during nanoindentation and scratching processes remain poorly understood and warrant further study. This investigation examines the plastic deformation of the $FeNiCoCrCu_x$ alloy caused by nanoindentation and scratching using molecular dynamics (MD) simulations. In particular, this paper investigates the effect of scratch depth and alloy compositions with respect to the nanoindentation and nanoscratch characteristics of the $FeNiCoCrCu_x$ HEA. The connection between the normal and friction forces with indentation depth and scratch distance is determined. The mechanisms of plastic deformation of the $FeNiCoCrCu_x$ HEA alloy are unveiled by examining the changes in microstructure and defects induced by the machining tool. Our findings aim to offer fresh perspectives on the characteristics of HEAs, thereby broadening their potential applications in industrial and technological sectors.

2. Computation method

Atomistic simulations based on molecular dynamics (MD) are conducted using the LAMMPS platform, which is abbreviated as Large-scale Atomic/Molecular Massively Parallel Simulator [28-30]. In this work, the nanoindentation and nanoscratching processes were simulated based on the configuration depicted in Figure 1. The model used for simulation is composed of a diamond template and a specimen composed of FeNiCoCrCu high-entropy alloy (HEAs). To construct the FeNiCoCrCu high-entropy alloy (HEA) sample, we create a face-centered cubic (FCC) workpiece with a lattice constant of 3.552 Å [11]. The specimen measures 130 Å along its length (L), 60 Å along its width (W), and 100 Å in height (H). The modeling process commences with the construction of a FCC lattice composed entirely of pure Fe atoms, possessing a lattice constant of 3.552 Å. This initial structure is carefully oriented such that the crystallographic directions [100], [010], and [001] are aligned with the X, Y, and Z axes, respectively. To obtain the target multicomponent alloy composition, Fe atoms within the matrix are stochastically and sequentially substituted with Ni, Cr, Co, and Cu atoms, following their respective molar ratios. To investigate the impact of Cu on the composition, we prepared five variations of $FeNiCoCrCu_x$ high-entropy alloys with different Cu concentrations (HEAs), where x denotes the Cu content in molar proportion, taking values of 0.2, 0.4, 0.7, 1.0, and 1.3. Additionally, the effects of scratching depth are examined in this study. We conducted our study using four samples with varying scratching depths of 1.0, 1.5, 2.0, 2.5 nm [31-32]. The molecular dynamics simulation is divided into two stages: indentation and scratching. During indentation, the abrasive tip moves downward along the Y-axis. In the scratching stage, the tip travels across the substrate in the X-axis direction at a steady velocity of 100 m/s in both phases.

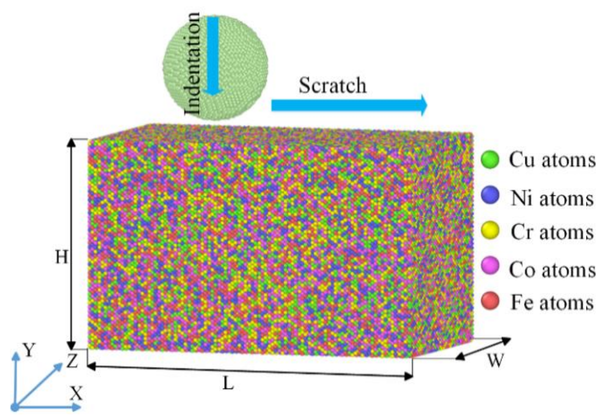

Figure 1. *Simulation model illustrating nanoindentation and nanoscratching processes in $FeNiCoCrCu_x$ HEAs*

We began by analyzing the effects of varying alloy compositions. The high-entropy alloys (HEAs) studied include $FeNiCoCrCu_{1.3}$ ($Cu_{1.3}$), $FeNiCoCrCu_{1.0}$ ($Cu_{1.0}$), $FeNiCoCrCu_{0.7}$ ($Cu_{0.7}$), $FeNiCoCrCu_{0.4}$ ($Cu_{4.0}$), and $FeNiCoCrCu_{0.2}$ ($Cu_{0.2}$). These alloys served as the basis for analyzing mechanical behavior during the nanoindentation and nanoscratching processes. Finally, we examined the effect of scratching depth at various levels: 1.0, 1.5, 2.0, 2.5 nm. The parameters for the MD simulation and the specimenare provided in Table 1. The interactions between Fe, Co, Cr, Ni, and Cu in the HEA material for the NIL simulation are modeled using the Embedded Atom Method (EAM) model [33]. These potential parameters have been widely used in prior research and have been shown to accurately replicate the mechanical and structural characteristics of FeNiCoCrCu [34-36]. The carbon-carbon interaction within the tool is neglected as the diamond tool is treated as an immovable object. The mutual interaction forces between the carbon atoms of the diamond tool and the substrate atoms are described using Lennard-Jones potentials [37].

To visualize and evaluate the outcomes, the Open Visualization Tool (OVITO) is used [38]. To detect dislocations and structural configurations, the Common Neighbor Analysis (CNA) method and Dislocation Analysis (DXA) are employed [39].

To gain a deeper insight into how the specimens undergo deformation during the indentation and nanoscratching processes, atomic shear strain as well as von Mises stress are computed. The VMS (von Mises stress) is calculated using the following formula [40, 41].

$$\sigma_{VMS} = \sqrt{3\left(\sigma_{xy}^2 + \sigma_{yz}^2 + \sigma_{zx}^2\right) + \frac{1}{2}\left[\left(\sigma_{xx} - \sigma_{yy}\right)^2 + \left(\sigma_{yy} - \sigma_{zz}\right)^2 + \left(\sigma_{zz} - \sigma_{xx}\right)^2\right]} \quad (1)$$

where σ_{ij} represents the virial stress term.

Using the von Mises shear strain (VMSS), the atomic shear strain is determined:

$$\eta_i^{VMSS} = \sqrt{\eta_{xy}^2 + \eta_{yz}^2 + \eta_{zx}^2 + \frac{1}{6} + \left[\left(\eta_{xx} - \eta_{yy}\right)^2 + \left(\eta_{xx} - \eta_{zz}\right)^2 + \left(\eta_{yy} - \eta_{zz}\right)^2\right]} \quad (2)$$

where η_{ij} denotes the tensor of atomic strain.

3. Result and discussion

3.1. Effect of alloy composition

This part investigates the impact of various FeNiCoCrCu alloy compositions on the underlying mechanisms during nanoindentation and nanoscratch processes. Five single crystal workpieces with varying compositions, namely FeNiCoCrCu$_{1.3}$ (Cu$_{1.3}$), FeNiCoCrCu$_{1.0}$ (Cu$_{1.0}$), FeNiCoCrCu$_{0.7}$ (Cu$_{0.7}$), FeNiCoCrCu$_{0.4}$ (Cu$_{0.4}$), and FeNiCoCrCu$_{0.2}$ (Cu$_{0.2}$), were meticulously prepared for this comprehensive study to investigate their structural and mechanical properties. The indentation and scratching tests were conducted at 300 K with a loading velocity of 100 m/s.

Figure 2(a-e) illustrates the load-time curves for the indentation and scratching stages in FeNiCoCrCu single crystals, highlighting the influence of varying compositional variations of alloys. At the onset of the process, the applied load during indentation steadily increases as the abrasive tip moves forward. This behavior occurs because the area of interaction between the tip and the substrate expands with increasing indentation depth. Consequently, atoms situated in the region of elevated strain undergo greater plastic deformation, causing the loading force to increase.

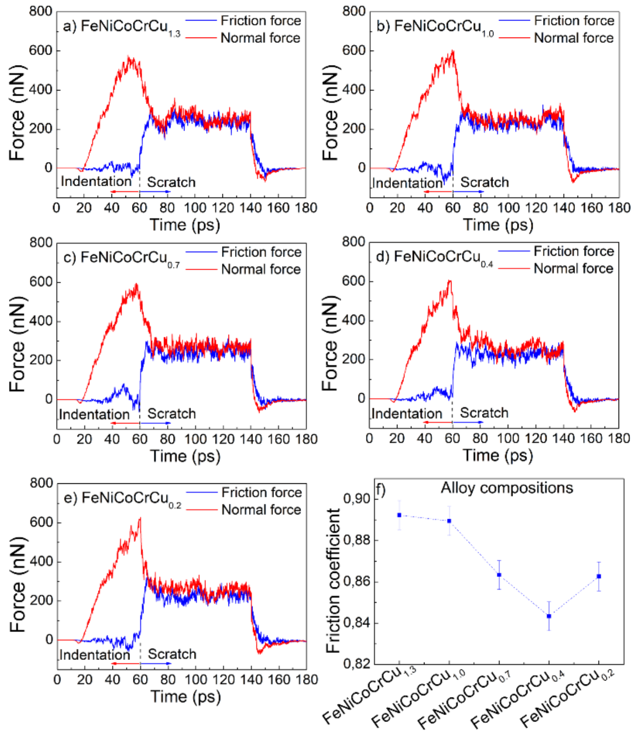

Figure 2. *The load-time curves (a-e) for the indentation and scratching stages, as well as the friction coefficient (f) during scratching, of FeNiCoCrCu$_x$ single crystals with varying alloy compositions*

In the indentation phase, the highest forces recorded during the process are as follows: 559.6 nN for Cu$_{1.3}$, 595.6 nN for Cu$_{1.0}$, 605.9 nN for Cu$_{0.7}$, 608.1 nN for Cu$_{0.4}$, and 628.7 nN for Cu$_{0.2}$. This trend reveals a significant increase in the peak indentation force as the copper composition decreases from Cu$_{1.3}$ to Cu$_{0.2}$. In the scratch phase, the highest forces measured are as follows: 267.1 nN for Cu$_{1.3}$, 276.6 nN for Cu$_{1.0}$, 281.7 nN for Cu$_{0.7}$, 289.2 nN for Cu$_{0.4}$, and 300.8 nN for Cu$_{0.2}$. This implies that a reduction in copper amount results in greater the alloy's hardness. As the copper content rises, the repulsive force exerted by the punch decreases, highlighting the softening effect observed in HEAs as a result of copper's relatively reduced Young's modulus. This finding aligns with the prior results reported by Mu et al. [42]. Figure 2(f) shows the friction coefficient η during the scratching phase of FeNiCoCrCu$_x$ single crystals with varying alloy compositions. The findings clearly show that the FeNiCoCrCu$_{1.3}$ alloy exhibits the highest η value among all compositions tested.

In Figure 3(a1-e1), the distribution of shear strain along the scratch path for FeNiCoCrCu single crystals with varying alloy compositions is presented. Each atom is color-coded according to its Von Mises shear stress (VMSS) magnitude during the scratching process. Notably, atoms experiencing significant shear are still positioned near the abrasive tip. As the scratching length increases, the zone exhibiting elevated VMSS values extends along the scratch path, particularly affecting the atoms ahead of the abrasive tip. Figure 3(a2-e2) illustrates how Von Mises stress (VMS) is distributed among atoms during scratching in FeNiCoCrCu single crystals with varying alloy compositions. The atoms are categorized by their Von Mises stress (VMS) values. Those positioned in ahead of the abrasive tip within the chip, along with those directly beneath the abrasive tip, experience the highest local stress.

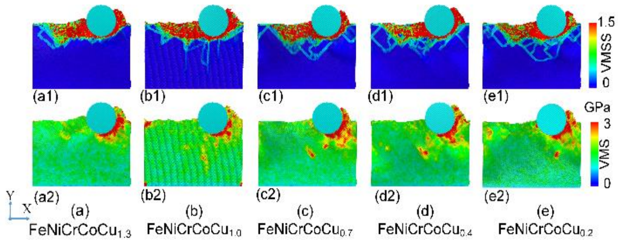

Figure 3. *Presents cross-sectional distributions of shear strain (a1-e1) and von Mises stress (a2-e2) at a specific scratch for FeNiCoCrCu$_x$ single crystals with varying alloy compositions*

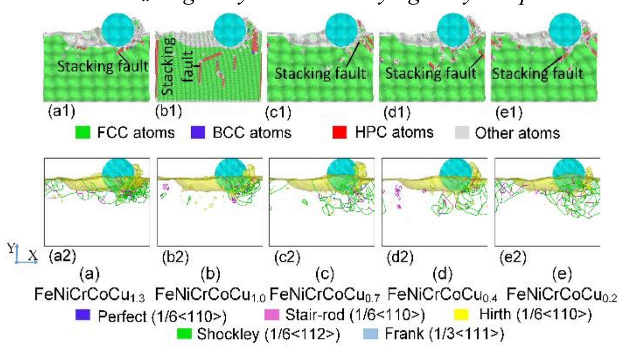

Figure 4. *The structural changes in FeNiCoCrCu$_x$ single crystal workpieces (a1-e1) and the dislocation network (a2-e2) for various alloy compositions*

Figure 4(a1-e1) illustrates the structural changes of FeNiCoCrCu$_x$ single crystal workpieces with varying alloy compositions. The results show that dislocations and stacking faults are present in each of the specimens. Additionally, disordered atomic structures distinctly emerge in the vicinity of the abrasive tip as a result of the peak shear stress encountered in this region. Figure 4 (a2-e2) shows the dislocation structure during the scratching process for various alloy compositions. The findings further reveal that Perfect and Shockley partial dislocations predominate in FeNiCoCrCu$_{1.3}$ single crystals, while Stair-rod and other types of dislocations are found to be least prevalent in FeNiCoCrCu$_{1.0}$ single crystals, highlighting the influence of composition on dislocation behavior.

Figure 5 depicts the change in dislocation length in FeNiCoCrCu$_x$ single crystal alloys during the indentation and scratching processes for various compositions of the alloy. The data show that overall dislocation length generally rises throughout both the indentation and scratching processes. However, there are significant decreases in dislocation length at certain points, particularly after the initial increase. In the early stage (indentation phase), when the indentation depth is large, the force acting on the workpiece becomes larger, causing stacking faults and increasing dislocations. In the scratch stage, dislocations are generated and interact with each other, causing the scratch forces to fluctuate during the scratching process. The increased dislocation density significantly promotes greater interaction between dislocations, resulting in the formation of dislocation pile-ups and tangles within the workpiece, serving as a critical mechanism for work hardening. Furthermore, the total dislocation length in the FeNiCoCrCu$_{0.2}$ alloy is notably higher compared to the other alloys observed during the indentation process.

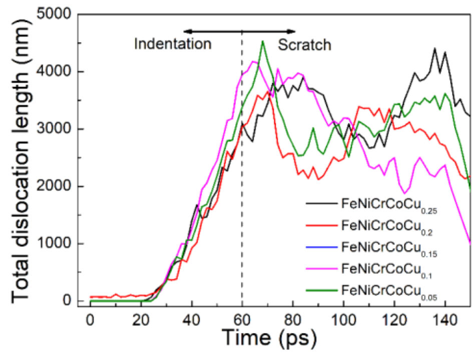

Figure 5. *Dislocation length of FeNiCoCrCu$_x$ single crystals alloy during indentation and scratching under various compositions*

These observations clearly indicate that alloy composition plays a crucial role in governing the deformation mechanisms during both nanoindentation and nanoscratch processes. As the Cu content decreases, the material exhibits higher resistance to plastic deformation, reflected in increased dislocation activity, more pronounced stacking faults, and greater overall dislocation density. Conversely, higher Cu content leads to a softening effect, reducing dislocation interactions and resulting in lower hardness and friction. Therefore, the variation in alloy composition directly modulates the evolution and interaction of defects, which ultimately determines the mechanical response of the material under applied load.

3.2. Scratch depth effect

To more effectively examine how scratch depth affects the deformation response of single-crystal FeNiCoCrCu$_{1.0}$ alloy, the processes are conducted at four different depths of 1.0, 1.5, 2.0, and 2.5 nm.

The load-time curves in Figure 6 (a) to (d) show significant variations in both friction and normal forces throughout the indentation and scratching phases, highlighting the dynamic interactions between the indenter and the material surface. As the indentation depth progresses from 1.0 nm (a) to 2.5 nm (d), there is a clear increase in the overall magnitude of both forces, indicating that deeper indentations lead to greater resistance and interaction forces. The shift from the indentation phase to the scratch phase is marked by distinct changes in the force profiles, with friction forces generally rising during scratching, suggesting enhanced material deformation.

Overall, these observations confirm the significant impact of indentation and scratching depth on the force responses of the FeNiCoCrCu single crystal. Figure 6(e) indicates the friction coefficient during both the indentation and scratching phases of the $FeNiCoCrCu_{1.0}$ alloy at various indentation and scratching depths. Consequently, the average friction coefficient rises as the depth increases [43]. This suggests that a higher friction coefficient at a depth of 2.5 nm during both indentation and scratching may result in increased tool degradation during the scratching process.

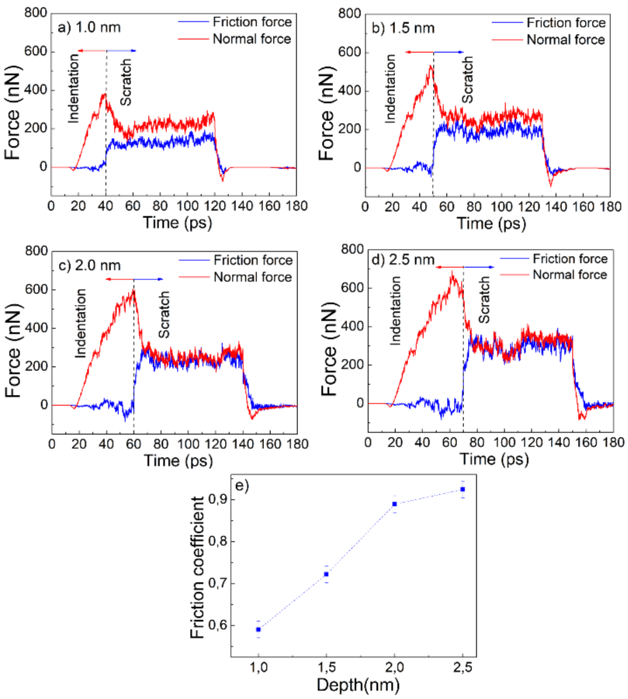

Figure 6. *The load-time curves (a-d) for indentation and scratch stages; friction coefficient (e) during the indentation and scratch of $FeNiCoCrCu_{1.0}$ single crystal under different indentation and scratch depths*

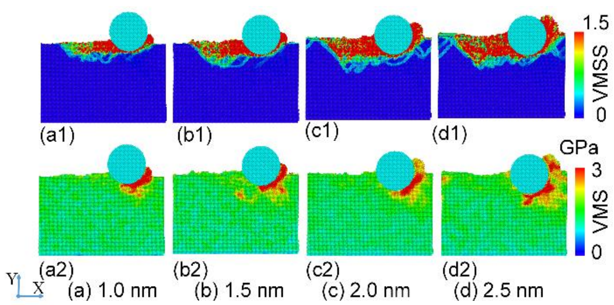

Figure 7. *Presents cross-sectional distributions of shear strain (a1-d1) and von Mises stress (a2-d2) at a specific scratch for $FeNiCoCrCu_{1.0}$ single crystals at different scratching depths*

Figure 7 illustrates the distribution of shear strain (a1-d1) and von Mises stress (a2-d2) across the cross-sections of the $FeNiCoCrCu_{1.0}$ single crystal at various scratching depths. In the shear strain distribution charts (a1-d1), atoms are color-mapped according to their Von Mises shear stress (VMSS) throughout the scratching process. It is evident that atoms in areas with elevated shear strain stay close to the abrasive tip. As the scratching length increases, the area with elevated VMSS values propagates along the scratch direction, particularly affecting the atoms positioned ahead of the abrasive tip. Localized strain concentrations are distinctly observed, with the level of strain increasing as the indentation depth increases. At a scratching depth of 1.0 nm (a1), the shear strain is observed to be relatively minimal. In contrast, for deeper indentations, such as at 2.5 nm (d1), the shear strain becomes significantly higher. The Von Mises stress distribution diagrams (a2-d2) further illustrate the material's stress response under indentation. As the depth increases, stress concentrations become more pronounced, particularly in areas aligned with high shear strain. This behavior reflects the mechanical response of the material to applied forces, where deeper indentations result in elevated stress levels.

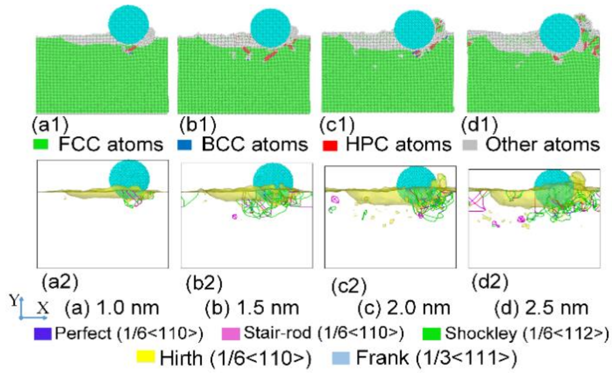

Figure 8. *The structural properties (a1-d1) and dislocation patterns (a2-d2) of the $FeNiCoCrCu_{1.0}$ workpiece under scratching at various depths*

The structural features (a1-d1) and distribution of dislocations (a2-d2) of the $FeNiCoCrCu_{1.0}$ workpiece are shown in Figure 8, illustrating the material's response to varying depths of scratching. In the structural characteristic diagrams (a1-d1), different atomic structures are represented by various colors. This representation highlights the complex microstructure of the $FeNiCoCrCu_{1.0}$ alloy and how it evolves under different loading conditions. As the cratching depth increases, the distribution of these atomic structures reflects significant changes in the material's organization and phase behavior. The dislocation distribution diagrams (a2-d2) provide insight into the movement and arrangement of dislocations within the material. At a depth of 1.0 nm (a2), dislocations appear relatively sparse, while deeper indentations, such as those at 2.0 nm (c2) and 2.5 nm (d2), show a denser network of dislocations. This increase in dislocation density suggests enhanced plastic deformation and material response as the depth of indentation and scratching increases. Dislocation analysis reveals that partial Shockley dislocations, Stair-rod dislocations, and various other types of dislocations are predominant across all cases. A key observation highlights the dominance of Perfect dislocations, Stair-rod partial dislocations, and others during scratching at 2.5 nm depth, while their presence is minimal at 1.0 nm.

Figure 9 shows how total dislocation length evolves over time in the FeNiCoCrCu HEA during indentation and scratching simulations at different depths. It gives insight into how deeper penetration affects dislocation dynamics. It points out that dislocation activity in FeNiCoCrCu HEA increases significantly with indentation depth. Larger depths generate longer and more dislocations due to the formation of larger plastic zones and stress concentrations. This behavior underscores the depth-dependent plasticity and strain hardening potential of the HEA.

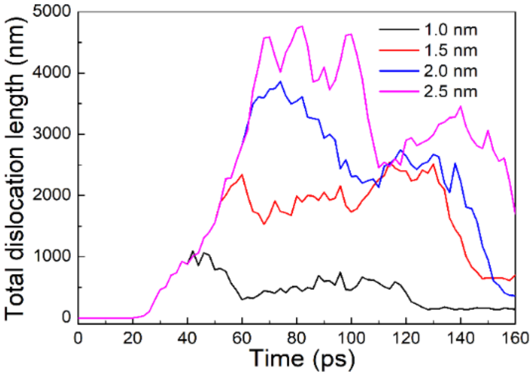

Figure 9. *Dislocation length of $FeNiCoCrCu_{1.0}$ alloy at a scratching phase under different depths*

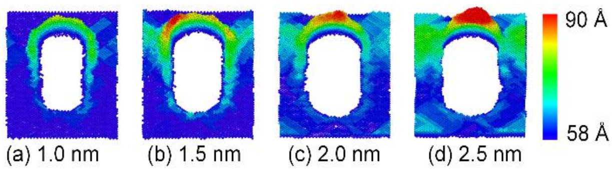

Figure 10. Atomic pile-up observed on the scratched regions of the FeNiCoCrCu1.0 alloy at various depths Figure 10 illustrates the pile-up of atoms along the scratch regions on the $FeNiCoCrCu_{1.0}$ alloy under different scratching depths. The atoms are color-coded based on their height. It is clear that the form of the pile-up varies across the various scenarios, with an asymmetric pile-up forming in all instances. As the scratch depth increases, the pile-up height also increases. Greater pile-up formation indicates faced by the abrasive tip encounters more significant resistance during scratching, resulting in increased friction. Consequently, the greatest pile-up height is noted at a scratching depth of 2.5 nm, resulting in a relatively higher frictional resistance of this alloy.

These findings clearly show that increasing the indentation depth intensifies the material's plastic response. At greater depths, the alloy exhibits stronger shear localization, higher stress accumulation, and denser dislocation networks. Various types of dislocations-particularly Shockley partials and stair-rod-are more active as the load increases, indicating that the material accommodates the applied stress through complex deformation patterns. The appearance of larger pile-up regions and greater dislocation activity confirms that deformation mechanisms such as dislocation glide and atomic rearrangement are highly sensitive to indentation depth. This clearly highlights depth as a key factor in controlling how the alloy responds mechanically under localized loading.

4. Conclusion

This study explores the impact of varying alloy concentrations and scratching depths on the material removal processes and deformation characteristics of $FeNiCoCrCu_x$ workpieces during indentation and scratching, using molecular dynamics simulations. The conclusions drawn from this study are as follows:

- The findings show that both the indentation and scratching forces rise as the copper content decreases and the scratch depths increase. Moreover, in all cases, the normal forces surpass the friction forces, resulting in friction coefficients lower than 1.0.

- A thorough examination of plastic deformation reveals that the distribution of stress and strain is primarily concentrated in the interface region between the abrasive tip and the workpiece.

- The findings from dislocation behavior analysis and the structural highlight that a key factor in the deformation process of single crystals is the dominance of stacking faults and dislocations. During the scratching process, a transition from the FCC phase to HCP, BCC, and amorphous phases is distinctly observed. Beneath the abrasive tip, dislocations are generated.

- The examination of pile-up morphology reveals that its shape varies significantly, which can be attributed to the differing atomic movements across the various orientations of the slip systems.

Acknowledgments: This research is funded by Ministry of Training and Education, Vietnam, under Project Number B2025.DNA.06.

REFERENCES

[1] E. P. George, D. Raabe, and R. O. Ritchie, "High-entropy alloys", *Nat. Rev. Mater.*, vol. 4, no. 8, pp. 515–34, 2019.

[2] B. Yin, F. Maresca, and W. A. Curtin, "Vanadium is an optimal element for strengthening in both fcc and bcc high-entropy alloys", *Acta Mater.*, vol. 188, pp. 486–91, 2020.

[3] W. R. Wang, W. L. Wang, S. C. Wang, Y. C. Tsai, C. H. Lai, and J. W. Yeh, "Effects of Al addition on the microstructure and mechanical properties of AlxCoCrFeNi high-entropy alloys", *Intermetallics*, vol. 26, pp. 44-51, 2012.

[4] F. Otto, A. Dlouhý, C. Somsen, H. Bei, G. Eggeler, and E.P. George, "The influences of temperature and microstructure on the tensile properties of a CoCrFeMnNi high-entropy alloy", *Acta Mater.*, vol. 61, no. 15, pp. 5743–5755, 2013.

[5] C. Han, Q. Fang, Y. Shi, S.B. Tor, C.K. Chua, and K. Zhou, "Recent advances in high entropy alloys for 3D printing", *Adv. Mater.*, vol. 32, no. 26, pp. 1-10, 2020.

[6] S. Picak *et al.*, "The low-cycle fatigue response of CoCrNiFeMn high entropy alloy with ultra-fine grain structure", *Acta Mater.*, vol. 205, pp. 116540, 2021.

[7] G. Jin *et al.*, "High temperature wear performance of laser-cladded FeNiCoAlCu high-entropy alloy coating", *Appl. Surf. Sci.,* vol. 445, pp. 113–122, 2018.

[8] A. S. Makarov, R. A. Konchakov, Y. P. Mitrofanov, M. A. Kretova, N. P. Kobelev, and V. A. Khonik, "A simple kinetic parameter indicating the origin of the relaxations induced by point(-like) defects in metallic crystals and glasses", *J. Phys. Condens. Matter.*, vol. 32, no. 49, pp. 495701, 2020.

[9] J. Menghani, A. Vyas, P. Patel, H. Natu, and S. More, "Wear, erosion and corrosion behavior of laser cladded high entropy alloy coatings – a review", *Mater. Today Proc.,* vol. 38, pp.2824–2829, 2021.

[10] S. Singh, S. M. Shaikh, P. Kumar M K, B. S. Murty, and C. Srivastava, "Microstructural homogenization and substantial improvement in corrosion resistance of mechanically alloyed FeCoCrNiCu high entropy alloys by incorporation of carbon nanotubes", *Materialia*, vol. 14, pp. 100917, 2020.

[11] O. R. Deluigi, R. C. Pasianot, F. J. Valencia, A. Caro, D. Farkas, and E.M. Bringa, "Simulations of primary damage in a High Entropy Alloy: probing enhanced radiation resistance", *Acta Mater.,* vol. 213, pp. 116951, 2021.

[12] V. T. Pham, T. N. Vu, D. B. Luu, V. T. Hoang, and Q. B. Tao, "Effects of temperature, punch angle, and loading velocity on mechanical properties of nanoimprinted FeNiCoCrCux high-entropy alloys", *Materials Today Communications*, vol. 38, pp. 107692, 2024.

[13] G. Luo *et al.*, "Microstructural evolution and mechanical properties of FeCoCrNiCu high entropy alloys: a microstructure-based constitutive model and a molecular dynamics simulation study", *Appl. Math. Mech.*, vol. 42, no. 8, pp. 1109–1122, 2021.

[14] Y. Cai, Y. Chen, Z. Luo, F. Gao, and L. Li, "Manufacturing of FeCoCrNiCux mediumentropy alloy coating using laser cladding technology", *Mater. Des.*, vol. 133, pp. 91–108, 2017.

[15] C. Shang, E. Axinte, W. Ge, Z. Zhang, and Y. Wang, "High-entropy alloy coatings with excellent mechanical, corrosion resistance and magnetic properties prepared by mechanical alloying and hot pressing sintering", *Surf. Interfaces*, vol. 9, pp. 36–43, 2017.

[16] A. Verma *et al.*, "High temperature wear in CoCrFeNiCux high entropy alloys: the role of Cu", *Scr. Mater.*, vol. 161, pp. 28–31, 2019.

[17] J. Joseph, N. Stanford, P. Hodgson, and D.M. Fabijanic, "Tension/compression asymmetry in additive manufactured face centered cubic high entropy alloy", *Scripta Mater.*, vol. 129, pp. 30–34, 2017.

[18] R. Sonkusare, R. Jain, K. Biswas, V. Parameswaran, and N.P. Gurao, "High strain rate compression behaviour of single phase CoCuFeMnNi high entropy alloy", *J. Alloys Compd.*, vol. 823, pp 153763, 2020.

[19] Q. Fang, M. Yi, J. Li, B. Liu, and Z. Huang, "Deformation behaviors of Cu29Zr32Ti15Al5Ni19 high entropy bulk metallic glass during nanoindentation", *Appl. Surf. Sci.*, vol. 443, pp. 122–130, 2018.

[20] C. Zhu, Z.P. Lu, and T.G. Nieh, "Incipient plasticity and dislocation nucleation of FeCoCrNiMn high-entropy alloy", *Acta Mater.*, vol. 61, pp. 2993–3001, 2013.

[21] C. Peng, F. Zeng, B. Yuan, and Y. Wang, "An MD simulation study to the indentation size effect of polystyrene and polyethylene with various indenter shapes and loading rates", *Appl. Surf. Sci.*, vol. 492, pp. 579–590, 2019.

[22] D. Q. Doan, T. H. Fang, and T. H. Chen, "Nanotribological characteristics and strain hardening of amorphous Cu64Zr36/ crystalline Cu nanolaminates", *Tribol. Int.,* vol. 147, pp. 106275, 2020.

[23] D. Q. Doan, T. H. Fang, and T. H. Chen, "Interfacial and mechanical characteristics of TiN/Al composites under nanoindentation", *Int. J. Solid Struct.*, vol. 226, pp. 1-17, 2021.

[24] J. Li, B. Liu, H. Luo, Q. Fang, Y. Liu, and Y. Liu, "A molecular dynamics investigation into plastic deformation mechanism of nanocrystalline copper for different nanoscratching rates", *Comput. Mater. Sci.*, vol.118, pp. 66–76, 2016.

[25] K. Sun, L. Fang, Z. Yan, and J. Sun, "Atomistic scale tribological behaviors in nano-grained and single crystal copper systems", *Wear*, vol. 303, pp. 191–201, 2013.

[26] P. Z. Zhu, C. Qiu, F. Z. Fang, D. Yuan, and X .C. Shen, "Molecular dynamics simulations of nanometric cutting mechanisms of amorphous alloy", *Appl. Surf. Sci.*, vol. 317, pp. 432–442, 2014.

[27] L. Zhang and Y. Shibuta, "Inverse Hall-Petch relationship of high-entropy alloy by atomistic simulation", *Mater. Lett.*, vol. 274, pp. 1-7, 2020.

[28] S. Plimpton, "Fast parallel algorithms for short-range molecular dynamics", *J. Comput. Phys.*, vol. 117, no. 1, pp. 1–19, 1995.

[29] D. Q. Doan, T. H. Fang, and T. H. Chen, "Microstructure and composition dependence of mechanical characteristics of nanoimprinted AlCoCrFeNi high-entropy alloys", *Sci. Rep.*, vol. 11, pp. 13680, 2021.

[30] D. Q. Doan, T. H. Fang, T. H. Chen, and T. X. Bui, "Effects of void and inclusion sizes on mechanical response and failure mechanism of $AlCrCuFeNi_2$ high-entropy alloy", *Eng. Fract. Mech.*, vol. 252, pp. 107848, 2021.

[31] K. E. Avila, S. Küchemann, I.A. Alhafez, and H.M. Urbassek, "Nanoscratching of metallic glasses–An atomistic study", *Tribol. Int.*, vol. 139, pp. 1–11, 2019.

[32] D. Q. Doan, T. H. Fang, A. S. Tran, and T. H. Chen, "High deformation capacity and dynamic shear band propagation of imprinted amorphous Cu50Zr50/crystalline Cu multilayered nanofilms", *J. Phys. Chem. Solids.*, vol. 138, pp. 109291, 2019.

[33] R. Pasianot, and D. Farkas, "Atomistic modeling of dislocations in a random quinary high-entropy alloy", *Comput. Mater. Sci.*, vol. 173, pp. 109366, 2020.

[34] H. Feng *et al.*, "Indentation-induced plastic behaviour of nanotwinned Cu/high entropy alloy FeCoCrNi nanolaminate: an atomic simulation", *RSC Adv.*, vol. 10, no. 16, pp. 9187–9192, 2020.

[35] O. Elgack, B. Almomani, J. Syarif, M. Elazab, M. Irshaid, and M. Al-Shabi, "Molecular dynamics simulation and machine learning-based analysis for predicting tensile properties of high-entropy FeNiCrCoCu alloys", *J. Mater. Res. Technol.*, vol. 25, pp. 5575–5585, 2023.

[36] J. Jiang, W. Sun, and N. Luo, "Atomic insights into effects of temperature and grain diameter on the micro-deformation mechanism, mechanical properties and sluggish diffusion of nanocrystalline high-entropy alloys", *Mater. Today Commun.*, vol. 33, pp. 104224, 2022.

[37] L. Xie, P. Brault, A. L. Thomann, and J. M. Bauchire, "AlCoCrCuFeNi high entropy alloy cluster growth and annealing on silicon: a classical molecular dynamics simulation study", *Appl. Surf. Sci.*, vol. 285, pp. 810–816, 2013.

[38] A. Stukowski, "Visualization and analysis of atomistic simulation data with OVITO–the Open Visualization Tool", *Model. Simul. Mater. Sci. Eng.*, vol. 18, no. 1, pp. 015012, 2009.

[39] D. Faken, and H. Jonsson, "Systematic analysis of local atomic structure combined with 3D computer graphics", *Comput. Mater. Sci.*, vol. 2, no. 2, pp. 279–286, 1994.

[40] D. Wang, J. Lee, K. Holland, T. Bibby, S. Beaudoin, and T. Cale, "Von mises stress in chemical-mechanical polishing processes", *J. Electrochem. Soc.*, vol. 144, no. 3, pp. 1121, 1997.

[41] V. T. Pham and T. H. Fang, "Interfacial mechanics and shear deformation of indented germanium on silicon (001) using molecular dynamics", *Vacuum*, vol. 173, pp. 109184, 2020.

[42] A. Mu *et al.*, "Nanoindentation into FeCoNiCrCu high-entropy alloy: an atomistic study", *Mater. Sci. Technol.*, vol. 37, no. 2, pp. 202–209, 2021.

[43] P. Liu, D. Sun, and Q. Wang, "An atomic-level understanding of the friction and wear behaviors of Ti2AlN/TiAl composite via MD simulations", *Tribol. Int.*, vol. 137, pp. 340-348, 2019.